ELSEVIER

1 June 1995

OPTICS COMMUNICATIONS

Optics Communications 117 (1995) 235–240

Self-stabilized holographic recording in $LiNbO_3$:Fe crystals

P.M. Garcia [a], K. Buse [b], D. Kip [b], J. Frejlich [a]

[a] *Laboratório de Óptica, Instituto de Física "Gleb Wataghin", Universidade Estadual de Campinas, 13083-970 Campinas-SP, Brazil*
[b] *Universität Osnabrück, Fachbereich Physik, Barbarastraße 7, D-49069 Osnabrück, Germany*

Received 13 August 1994; revised version received 18 November 1994

Abstract

We describe the self-stabilized holographic recording in Fe-doped $LiNbO_3$ crystals reaching almost 100% diffraction efficiency using weak interfering beams of 514.5 nm wavelength, even for relatively low light pattern modulation values. The evolution of the recording process is shown to be adequately described by a simple mathematical formulation based on Kogelnik's coupled-wave theory in spite of the dynamic nature of the recording process. Crystal parameters computed from this experiment are compared to the available data from literature.

1. Introduction

Self-stabilized techniques have been extensively used for holographic recording in $Bi_{12}SiO_{20}$(BSO)-type photorefractive crystals [1] exhibiting low diffraction efficiency and 90°-shifted holograms. In these conditions self-diffraction effects are negligible or may just result in the variation of the light pattern modulation along the crystal thickness. This is not valid for doped $LiNbO_3$ and photovoltaic crystals in general, that are known to reach large diffraction efficiencies and to produce 180°-shifted holograms. This is the usual case for doped $LiNbO_3$ with a grating vector along the *c*-axis as has been shown by precise microphotometric investigations [2] and by two-beam coupling measurements [3]. In these crystals phase-coupling effects are expected if the recording is performed with interfering beams of different intensity that lead to a progressive shifting or bending in the hologram phase planes throughout the crystal thickness [4–7]. Such holograms will be here referred to as "bended" holograms. The question arises whether self-stabilized recording may ever be possible in these conditions.

In this paper we report the successful use of self-stabilized holographic recording in $LiNbO_3$ crystals using weak recording beams (a few mW/cm^2 at λ = 514.5 nm) of wide different input beam intensity ratios. An almost 100% diffraction efficiency is reached in these conditions that is indefinitely kept as long as the stabilization system is on. We also show that a simple mathematical model based on Kogelnik's coupled-wave theory [8] adequately describes the diffraction efficiency evolution in spite of the dynamic nature of the recording process that may lead to phase-coupling effects [4].

2. Theory

The stabilized recording setup in this experiment is similar to the already described one for BSO-type crystals [1] and is shown in Fig. 1. The basic procedure is phase modulation (with amplitude $\psi_d \ll 1$) of one of the interfering beams (S in this case), with

SSDI 0030-4018(95)00157-3

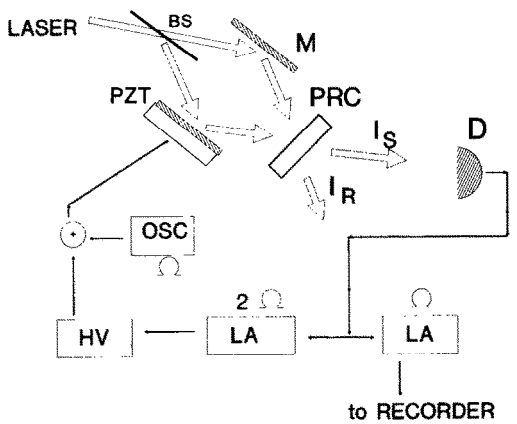

Fig. 1. Self-stabilized recording setup. M: mirror, PZT: piezoelectric supported mirror, BS: beamsplitter, PRC: $LiNbO_3$ crystal, D: detector, LA: lock-in amplifier, HV: high voltage amplifier for PZT, OSC: oscillator

a frequency Ω that is much higher than the frequency response of the crystal. The overall irradiance I_S along the S-direction at the crystal output results from the interference of the modulated transmitted S-beam with the diffracted R-beam. I_S is written following the simple Kogelnik's formulation for a refractive-index grating that is ϕ-shifted to the interference pattern of light [8,9]:

$$I_S = |S_0 \cos(\kappa d)\exp[i\psi_d \sin(\Omega t)] + i\exp(i\phi) R_0 \sin(\kappa d)|^2, \quad (1)$$

with

$$\kappa d = \frac{\pi n_1 d}{\lambda \cos\theta'}, \quad (2)$$

$$n_1 = -n_{\text{eff}}^3 r_{\text{eff}} E_{\text{sc}}/2, \quad (3)$$

where $S_0 = (I_S^0)^{1/2}$, $R_0 = (I_R^0)^{1/2}$, and the corresponding input irradiances are I_S^0 and I_R^0. The term $\exp[i\psi_d \sin(\Omega t)]$ accounts for the phase modulation of beam S, d is the crystal thickness, λ the light wavelength, θ' the incidence angle inside the crystal, n_{eff} the corresponding (ordinary or extraordinary) bulk refractive index, r_{eff} the effective electrooptic coefficient, and E_{sc} is the amplitude of the modulated space charge field. The development of Eq. (1) allows to find the expressions for the amplitude of the first (I^{Ω}) and the second ($I^{2\Omega}$) harmonics in Ω:

$$I^{\Omega} = \psi_d I_0 (m/2) \sin(2\kappa d) \sin(\varphi), \quad (4)$$

$$I^{2\Omega} = (\psi_d/2)^2 I_0 (m/2) \sin(2\kappa d) \cos(\varphi), \quad (5)$$

where absorption effects are neglected, $\varphi = \phi + 90°$, $m = 2(I_S^0 I_R^0)^{1/2}/(I_S^0 + I_R^0)$ is the pattern of light modulation, and $I_0 = I_S^0 + I_R^0$. In crystals with dominating photovoltaic field, as in the present case, this field is more than two orders of magnitude larger than the diffusion field. From a simple estimation, not taking into account the dynamic energy transfer [10], we get $\phi \approx 180°$ for the expected phase shift with an error smaller than 1 percent. So $\varphi = -90°$ and we get $I^{2\Omega} = 0$. Therefore $I^{2\Omega}$ can be used as error-signal for operating a negative feedback loop acting on the piezoelectric-supported mirror in the holographic setup in Fig. 1. This technique is called self-stabilized recording because the recorded hologram itself is used as a reference for the stabilization process: any perturbation in the setup will shift φ away from its stationary $\varphi = -90°$ condition thus making $I^{2\Omega} \neq 0$ and resulting in a voltage on the piezoelectric so that the PZT-supported mirror will move to compensate for the perturbation until the stable equilibrium $I^{2\Omega} = 0$ condition is restored. There are two stable equilibrium conditions [11] for $I^{2\Omega} = 0$ depending on whether the pattern of light is fixed at $\phi = 180°$ or at $\phi = 0°$ to the hologram being recorded. One position produces constructive recording and the other one erasure. We may switch from one condition to the other by just changing the sign of the $I^{2\Omega}$ signal at the corresponding lock-in amplifier output. Once the constructive recording condition is chosen and $\kappa d = \pi/2$ ($\eta = \sin^2(\kappa d) = 1$) is reached, any further increase in κd will produce a change in the sign of $I^{2\Omega}$ in Eq. (5) leading to stabilized erasure. Consequently κd will drop below the limiting $\pi/2$ value and the constructive holographic recording will start again, and so on. That is why the system is supposed to be in stable equilibrium at $\eta = 1$ and will stay at this point as long as the stabilization is on. As mentioned above, $LiNbO_3$ exhibits strong phase-coupling effects that are expected to result in bended holograms [4], and in this case it is not obvious that the simple relations above will still verify and enable operating the stabilization setup.

The time evolution of signal $V^{\Omega} = k_D I^{\Omega}$ (k_D = 24.7 $V\,cm^2/mW$ is the photodetector sensitivity) is assumed to be described by an exponential time evolution for the amplitude of the electric space charge field in the crystal, in which case Eq. (4) can be written as

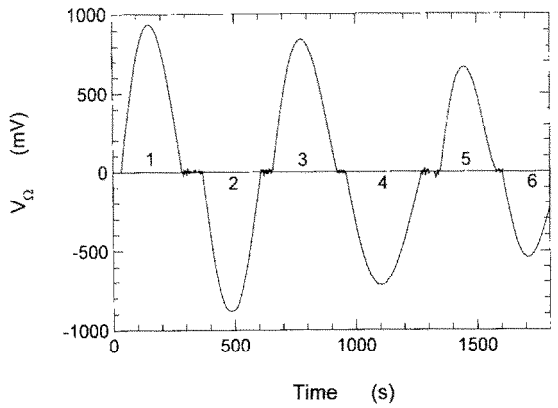

Fig. 2. Measured first harmonic evolution during self-stabilized holographic recording and erasure in $LiNbO_3$:Fe (sample SC#1, extraordinary polarization, I_1 = 5.1 mW/cm^2 and I_2 = 10.0 mW/cm^2). The odd cycles correspond to holographic recording, whereas the even cycles correspond to holographic erasure. Diffraction efficiency measured at the end of the cycles: $\eta \approx 1$ and $\eta \approx 0$, respectively, for the odd and even cycles.

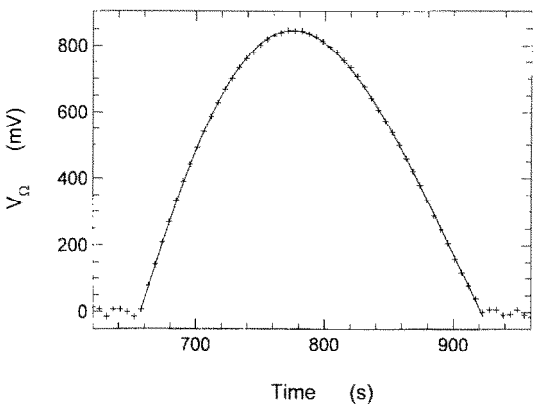

Fig. 3. Fit of Eq. (6) (continuous curve) to the experimental data (crosses) from the cicle number 3 in Fig. 2.

$$V^{\Omega}(t) = A\sin\{B[1-\exp(-t/\tau)]\}, \tag{6}$$

where

$$A = k_D \psi_d I_0 m/2, \tag{7}$$

$$B = \frac{\pi d n_{eff}^3 r_{eff} m E_{sc}^0}{\lambda \cos\theta'}, \tag{8}$$

$$\tau = \epsilon_{33}^{st}\varepsilon_0/\sigma, \tag{9}$$

where ϵ_{33}^{st} is the static dielectric constant and ε_0 is the electric permittivity of vacuum. The space charge field in Eq. (8) can be written in terms of the photovoltaic field E_{ph} so that

$$E_{sc}^0 = E_{ph} = \kappa_{ph} I/(\sigma d), \tag{10}$$

where κ_{ph} is a photovoltaic transport coefficient [12], σ the photoconductivity and I the effectively absorbed irradiance [13].

3. Experiment

Self-stabilized holographic experiments were carried out using different Fe-doped $LiNbO_3$ crystals with their c-axis in the incidence plane and parallel to the grating vector K. An interference pattern of light of λ = 514.5 nm was projected onto the whole crystal surface, where the incidence angle in air was $\theta = 16°$.

The V^{Ω} signal was measured along the S-direction behind the crystal and its evolution was registered during the holographic recording whereas the $V^{2\Omega} = 0$ (and consequently $\varphi = -90°$) condition was kept fixed by the action of the stabilization system. The evolution of V^{Ω} in non-stabilized conditions was always strongly perturbated and non-reproductible for the long time of recording required by the rather low intensity of the recording beams and environmental conditions in our experiments. The experimental evolution of V^{Ω} at the photodetector output during self-stabilized recording is plotted in Fig. 2 for the sample SC#1 (thickness d = 1.78 mm) using extraordinarily polarized Ar^+ laser beams. At the end of the first recording cycle, the beam R was momentarily switched off in order to measure the diffraction efficiency of the recorded grating and it was verified that almost all light (more than 95%) along the S-beam was diffracted showing that, within experimental uncertainties, the $\eta \approx 1$ condition was reached. This condition was actually verified to hold indefinitely as long as the stabilization was on, as shown by the trace at the end of the recording cycle, in agreement with the theoretical discussion above. After some time we changed the sign of the feedback signal at the output of the 2Ω-tuned lock-in amplifier in the stabilization loop. In this case the pattern of light is 180°-shifted from its former position and stabilized holographic erasure proceeds. Stabilized recording and erasing were alternatively performed several times. At the end of each recording cycle (odd numbers in Fig. 2) we measured $\eta \approx 1$ whereas at the end of the erasure ones (even numbers in Fig. 2) it was

Table 1
Experimental results

Sample	Pol.	I_S^0 (mW/cm^2)	I_R^0 (mW/cm^2)	αd	A (V)	B (rad)	τ (s)	$\mathcal{S}$ (10^{-11} m^3/J) Exp.	Theor.
SC#1	ORD	4.8	9.6	1.46	4.0	4.4	1360	0.29	0.33
	EXT	5.1	10.0	0.95	8.4	8.7	590	1.51	
TO2-12	EXT	9.5	5.0	0.19	18.2	5.7	2530	0.77	1.05
751-8	EXT	5.8	0.8	0.99	–	7.8	1760	1.46	

$\eta \approx 0$. Note that the maxima for the successive cycles are decreasing, probably due to the increasing amount of light scattered away from the crystal. The lowering in the successive maxima follows an exponential law where the time constant is 950 s for our experimental conditions. Fig. 3 shows a fit of the Eq. (6) (continuous curve) to the experimental data (crosses) from cycle number 3 of Fig. 2. All other cycles in Fig. 2 showed a good agreement with the theory as that one plotted in Fig. 3. From this fit, parameters A, B and τ were computed and displayed in Table 1.

The same experiment was repeated with the same sample using ordinarily polarized light. The time evolution of V^{Ω} in this case was slower probably due to the larger bulk ordinary absorption coefficient, but showed the same good agreement with the theoretical model. A similar good fit was obtained for a different sample (labelled TO2-12, 0.94 mm thick) using extraordinarily polarized light. This sample exhibits a lower absorption coefficient and looks much more uniform compared to sample SC#1.

Another experiment was performed using a third sample (751-8, 0.85 mm thick) and higher input beam ratio (≈ 7.3) of extraordinarily polarized light. Differently than the above reported experiments, in this case a sensible drift of the PZT-supported mirror was detected: a progressive shift away from the $V^{2\Omega} = 0$ condition that had to be periodically reset back to zero during recording. Nevertheless in these conditions the stabilized recording did work, $\eta \approx 1$ (with a precision better than 5%) was also reached and the experimental time evolution of the V^{Ω} signal shown in Fig. 4 did adequately fit Eq. (6) almost as well as for the other experiments described above.

Because of the high Bragg selectivity of the thick recorded holograms in this work, only a single diffracted order was detected behind the sample in these experiments. The diffraction efficiency was always computed as the diffracted beam intensity over the diffracted plus transmitted beams intensities behind the crystal. In this way the recorded hologram is better characterized because bulk absorption, uniformly scattered light and Fresnel reflections need not be considered. It is also necessary to point out that non-stabilized experiments were also carried out but were not registered because they were always strongly perturbated and non reproductible leading to much lower diffraction efficiencies.

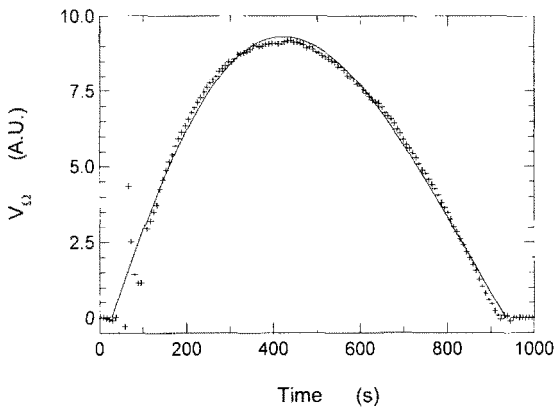

Fig. 4. Fit of Eq. (6) (continuous curve) to the experimental data (crosses) during self-stabilized holographic recording (sample 751-8, extraordinary polarization, $I_1 = 5.8$ mW/cm^2 and $I_2 = 0.8$ mW/cm^2). The noisy signal at the beginning was due to the preliminary adjustment of operating conditions.

4. Discussion

The parameters B and τ are related to fundamental crystal constants. In fact the so called holographic sensitivity $\mathcal{S} = n_{\text{eff}}^3 r_{\text{eff}} \kappa_{\text{ph}} / (2\epsilon_{33}^{\text{st}} \varepsilon_0)$ defined as the refractive index variation per unit absorbed energy in the unit crystal volume for unit incident light pattern

Table 2
Material parameters

$n_o = 2.33$	[17]
$n_e = 2.25$	[17]
$r_{13} = 8.6 \times 10^{-12}$ m/V	[18]
$r_{33} = 30.8 \times 10^{-12}$ m/V	[18]
$\epsilon_{33}^{st} = 32$	[18]
$\kappa_{ph} \approx 1.7 \times 10^{-11}$ m/V	[19]

modulation, at the initial recording stage [14], can be computed from the experimental parameters B and τ

$$S = \frac{B}{\tau} \frac{\lambda \cos\theta'}{2\pi m I}. \tag{11}$$

The S values computed from our experimental data are reported in Table 1 and are shown to be in good agreement with the theoretical values computed from the available data in the literature listed in Table 2. Note that the theoretical development in this paper is concerned with the so called first harmonic approximation that is verified for $m \ll 1$ but not necessarily valid for the $m \approx 1$ value in most of the experiments described in this paper, a fact that may explain the lack of a better agreement between experimental data and theory in Table 1. It must be also pointed out the presence of a strong light scattering effect that may have a sensible effect on the measured response time τ_{sc} [15] and may also interfere with a better agreement with theory.

Symmetry considerations show that dynamic holographic recording in photovoltaic crystals leads to nonbended holograms as long as the recording is carried out with interfering beams of equal intensity. Neither energy nor phase coupling are supposed to occur in these conditions so that Kogelnik's formulation does hold as was already experimentally verified [16]. In this case the $V^{2\Omega} = 0$ condition is verified. This is not the case of the experiments reported in this paper where input intensity beam ratios vary from $\sim 2 \sim 7$ (see Table 1) and therefore bended holograms are expected to occur. However, our results for different samples and light polarization states do fit very well the simple Kogelnik's diffraction efficiency formulation with the time evolution recording process being just represented by a simple exponential relation. This simple model does also explain the fact that the $\eta = 1$ condition can be indefinitely kept in stabilized recording mode. On the other hand the continuous drift trend of $V^{2\Omega}$ verified in the experiment for the highest interfering beam ratio (~ 7.3 with $m \approx 0.65$) shows that the $V^{2\Omega} = 0$ condition is not the characteristic one for the equilibrium state. In fact $V^{2\Omega} \neq 0$ is predicted [7] from dynamic coupled-wave theory even if $\phi = 180°$ is strictly verified, so that we assume that hologram bending is the reason for the small drift in the self-stabilized second harmonic. This assumption is reinforced by the fact that such a drift is only sensible for large interfering beams intensity ratios, where hologram bending effects are also supposed to increase [7,16]. On the other hand there is also the possibility that a hologram phase-shift slightly different from 180° be the cause of the second harmonic drift. This latter possibility, however, is not supported by any experimental evidence in this work.

The actively imposed $V^{2\Omega} = 0$ condition allows to record the hologram in such a way to reach $\eta = 1$ even in the presence of a light pattern modulation m considerably lower than 1. It is not clear yet why a good experimental agreement with the Kogelnik's formulation is verified in conditions where hologram bending is expected to occur. Experimental evidences in this work indicate that the imposed $V^{2\Omega} = 0$ condition does apparently prevent hologram bending during recording.

5. Conclusions

We have shown that self-stabilized holographic recording in $LiNbO_3$ leads to an almost 100% (within the limits of experimental uncertainties) diffraction efficiency that can be kept at this level as long as stabilization is operating, even for low light pattern modulation coefficients. The simple Kogelnik's coupled-wave theory is shown to describe fairly well the recording process in self-stabilized regime. Experimental evidences are here reported showing that self-stabilized recording may prevent hologram bending in $LiNbO_3$.

The stabilized recording procedure and the results described in this paper may both help developing new applications and provide a new technique for studying holographic recording in photovoltaic crystals.

Acknowledgements

This research was partially supported by Volkswagen-Stiftung (Germany) and Brazilian National Council for Scientific and Technological Research - CNPq.

References

[1] P.A.M. dos Santos, L. Cescato and J. Frejlich, Optics Lett. 13 (1988) 1014.
[2] R.A. Rupp, Appl. Phys. B 41 (1986) 153.
[3] R.A. Rupp, R. Sommerfeldt, K.H. Ringhofer and E. Krätzig, Appl. Phys. B 51 (1989) 364.
[4] N.V. Kukhtarev, V.B. Markov, S.G. Odulov, M.S. Soskin and V.L. Vinetskii, Ferroelectrics 22 (1979) 949.
[5] R.S. Cudney, G.D. Bacher, R.M. Pierce and J. Feinberg, Optics Lett. 17 (1992) 67.
[6] R. Hofmeister, A. Yariv, A. Kewitsch and S. Yagi, Optics Lett. 18 (1993) 488.
[7] J. Frejlich, Optics Comm. 107 (1994) 260.
[8] H. Kogelnik, Bell Syst. Tech. J. 48 (1969) 2909.
[9] D.L. Staebler and J.J. Amodei, J. Appl. Phys. 43 (1972) 1042.
[10] N.V. Kukhtarev, V.B. Markov and S.G. Odulov, Optics Comm. 23 (1977) 338.
[11] J. Frejlich, L. Cescato and G.F. Mendes, Appl. Optics 27 (1988) 1967.
[12] A.M. Glass, D. von der Linde and T.J. Negran, Appl. Phys. Lett. 25 (1974) 233.
[13] R. Grousson, M. Henry and S. Mallick, J. Appl. Phys. 56 (1984) 224.
[14] P. Günter, Photorefractive Effects and Materials - Topics in Applied Physics: Photorefractive Materials and Their Applications I, ed. P. Günter and J.-P. Huignard, Vol. 61 (Springer, Berlin, 1988) pp. 7–73.
[15] E.S. Maniloff and K.M. Johnson, J. Appl. Phys. 73 (1993) 541.
[16] A.A. Freschi and J. Frejlich, J. Opt. Soc. Am. B 11 (1994) 1837.
[17] L. Arizmendi, J. Appl. Phys. 64 (1988) 4654.
[18] A. Yariv, Optical Eletronics, 3rd Ed. (HRW International Edition, 1985).
[19] R. Sommerfeldt, L. Holtman, E. Krätzig and B.C. Grabmaier, Phys. Stat. Sol. (a) 106 (1988) 89.